



# A Methodology for Glaucoma Disease Detection Using Deep Learning Techniques

Fatima Ghani<sup>1</sup>, Mian Usman Sattar<sup>2</sup>, Hamza Wazir Khan<sup>3</sup>, Mehak Narmeen<sup>4</sup> and Ahsan Mehmood<sup>5</sup>

<sup>1,3,4</sup>Department of Information Systems, University of Management and Technology, Lahore, Pakistan.

<sup>2</sup>Department of Management, School of Business, Beaconhouse National University, Lahore, Pakistan

<sup>5</sup>Department of Information and technology, Central Queensland University, Melbourne, Australia

E-mail address: [f2018313030@umt.edu.pk](mailto:f2018313030@umt.edu.pk), [usman.sattar@bnu.edu.pk](mailto:usman.sattar@bnu.edu.pk), [hamza.khan@umt.edu.pk](mailto:hamza.khan@umt.edu.pk), [f2017313005@umt.edu.pk](mailto:f2017313005@umt.edu.pk), [ahsan.mehmood@cqumail.com](mailto:ahsan.mehmood@cqumail.com)

Received 19 Aug. 2020 , Revised 24 Oct. 2021 , Accepted 4 Jan. 2022 , Published 20 Jan.2022

**Abstract:** The advancement of computer technology and the needs of image processing is spreading in a wide range of applications. There are many techniques in image processing and one of the major techniques is Image classification. In the literature, we have reviewed many methods of machine learning used on Glaucoma pictures by different researchers. There are different machine learning algorithms include C4.5, the Naive Bayes Classifier, and Random Forest. These algorithms of machine learning cannot more reliably diagnose glaucoma disease. We have developed an architecture focused on the methodology of Deep Learning (DL), which is a Convolution Neural Network (CNN) for the classification of Glaucoma diseases. We used two different deep learning neural networks such as the Inception-V3 and the Vgg-16 Model for Glaucoma classification and identification purposes. We have obtained 508 Glaucoma images belonging to 25 groups from the Joint Shantou International Eye Center (JSIEC), Shantou City, Guangdong Province, China, Joint Shantou Foreign Eye Centre. Since uploading the images, we've increased the provided data set and rendered the 1563 training and testing data collection pictures. The downloaded data set is not labelled, so we wanted a named picture data set for our research in deep learning. But we have labelled both photos with the class name of the disease after the augmentation. We've also used two deep neural network models Inception-V3 and Vgg-16, which are supervised learning methods for classification arrangements. Such structures require operating processes that need to learn to use previous knowledge, make judgments about it, and fix it if any errors arise. We have used the Dropout: 0.5, Library: cv2, NumPy, Enjoinment API: Keras, TensorFlow, Loss Function: Cross-Entropy, Learning Rate: Adam, Fully Connected: SoftMax Activation Function with 2 Layer, Average Pooling: 4 Layer, Convolution: Tanh Activation Function with 2 Layer. Taking into consideration the success findings collected, it is shown that the pre-trained Inception-V3 model has the best classification accuracy with 90.01 percentage than Vgg-16 model which has an accuracy of 83.46 percent respectively.

**Keywords:** Glaucoma images; machine learning; convolutional neural network; classification; Inception-V3 and Vgg-16

## 1. INTRODUCTION

The advancement of computer technology and the needs of image processing are spreading in a wide range of applications [1]. There are a lot of techniques in Image Processing, and Image Classification is one of them. People have used many image classification methods, and there is no one specific solution for image classification. The image classification's primary target is to find the features in the depth of the image and detect the disease, which is called the label class. Classification is the way to divide an image into many parts or levels from which we take our target area. Thus, we stop classification at that point when we take our interested part from it. We have studied different

researches where the author has used Conditional Random Field to improve the state of the art by transfer labels in sketches and classification [2]. The author has used a selective search method for object recognition in multiple locations in a single picture [3]. The author presented an integrated framework, OverFeat in Convolutional Networks for localization, detection, and classification by boundaries [4]. He used color analysis for face location by region classification with a skin-color map [5]. The author used FaceNet for learning a mapping from the images of face to measure the similarity between faces [6].

Glaucoma has no treatment, and it is one of the main

reasons for blindness and visual disability across the world. In the early stages of these diseases, it does not cause blindness. The loss of vision can be prevented if glaucoma is diagnosed at an early stage. So, it can be said that glaucoma is the salient chronic eye disease. The number of victims of this chronic disease increases day by day, more specifically in urban areas. According to recent research, it was estimated that by 2020, the number of victims of this disease would reach 79 million. So, for its prevention, and first-level screening test is required [7].

The eye screening process can be done more efficiently by ophthalmologists, and a better result can also be extracted to providing a cost-effective solution for patients. Using an in-depth learning approach, we can reduce the time and effort wasted on testing and analyzing glaucoma. For differentiating between the glaucoma retinal image and healthy image of Glaucoma, the Computer Aided Diagnostics (CADx) system should be implemented in clinics and hospitals. It will help the ophthalmologists to differentiate between the healthy and damaged retina. "Fig. 1" shows that the retina's boundary is affected due to glaucoma eye disease.

PeriPapillary Atrophy (PPA) is another detector for the indication of the glaucoma diseases in the eye. The change in the boundary of the disc as intensity adjoining can be observed in the case of the PPA effect, as shown in "Fig. 2".

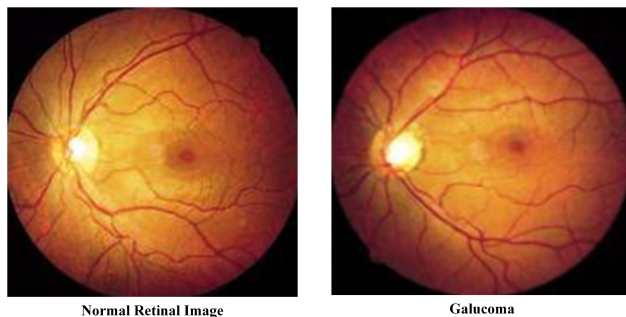


Figure 1. An example of visually presented glaucoma: (a) standard retinal image, (b) glaucoma

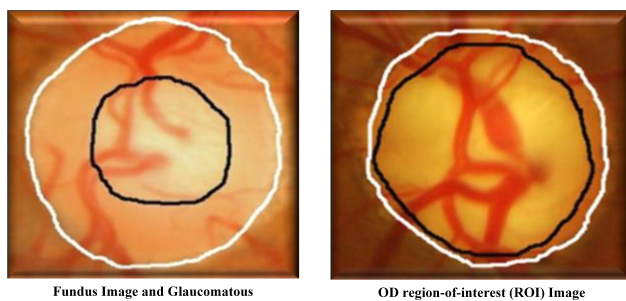


Figure 2. Sample of ordinary (a) fundus image and glaucomatous (b) OD region-of-interest (ROI) image

In early research, the authors presented an automatic so-

lution and the classification of this chronic disease through the Cup to Disc Ratio (CDR). Thus, we can say that it is challenging to classify the retina in the disc's boundary. So, after extraction of the features, if we are not using the retina regions' classification, then many image processing techniques are required. So, as we do not have any expertise to select the discriminative features after defining the image features, we can say that glaucoma detection is a difficult task by using the CADx systems for ophthalmologists [8]. The image features around the retina region, a glaucoma eye disease can be detected instead of using the classification approach. The need to accurately recognize cup and disc borders can be reduced by using a technique in which it can be pre-assumed that morphological change in the retina caused by the disease. So, in-depth learning basic features can be automatically extracted without expertise in a specific image processing [9].

#### A. Contribution of the Research

This research aims to identify the disease with a hybrid method that includes a deep neural network. And in the calculation of depletion, accuracy, precision, recalls, and F1, the proposed model's performance will be measured. This research contributes significantly to the deep neural learning network and compares the accuracy of two CNN models and finds which model has the highest accuracy for detecting the Glaucoma disease.

In this paper, we have six sections. In the 1st section, we have discussed the brief introduction of our manuscript. In the 2nd section, we have discussed the literature review related to our Glaucoma disease detection. In the 3rd section, we have a research methodology with ten subsections. In the 4th section, we have discussed the results and discussion, where we have described the statistical and graphical results of CNN models. In the 5th section, we have discussed the conclusion of our manuscript, and in the last section, we have discussed the future work of the paper.

## 2. LITERATURE REVIEW

This section explores several main principles and models used for Deep learning and neural networks to identify pictures and recognize artifacts and sketches. One of these Deep Learning models is CNN (Convolutional Neural Network), a learning algorithm that is the finest and widely used picture classification. This section includes much of the significant and better learning methods for picture classification such as ACO, OverFeat, MCG, Invention V-3, and Vgg-16. This section explores several of the earlier approaches proposed by researchers about their learning performance, which produced encouraging results.

The performance of glaucoma detection can be enhanced by applying CNN, but this performance depends on the number of labeled samples available for its training stage. Despite the lack of labeled samples, RIM-ONE (database) experimental results show the suggested algorithm [10].



This paper explores the potential usage of deep learning to establish artificial feature learning strategies in colored retinal fundus images to identify glaucoma. A fully-automated framework based on the convolution neural network (CNN) is developed. The author has 88.2 percent accuracy, efficiency, and versatility relative to the current state-of-the-art but at slightly lower computing costs [11].

Glaucoma is a neurodegenerative disorder that is considered unique and one of the most widely recorded causes of vision loss. Nerve degeneration is a non-respecting process, and early disease diagnosis is a requirement for keeping away from long-lasting vision impairment. This paper focuses on the various forms of diagnosis being used and suggested by specific scientists for glaucoma's recognition. This report also analyzes the results and treatment-related work [12].

Computer-aided diagnostics (CAD) is a non-invasive technique that uses digital fundus images to detect glaucoma in its early stage. An eighteen-layer CNN framework is efficiently equipped to remove robust features. With 1426 fundus pictures, the author has achieved 98.13 percent of the maximum accuracy. Our study findings demonstrate the method's robustness and can be used to verify clinicians' decisions [13].

The author explores how to blend profound information with retinal fundus photos to diagnose glaucoma using a deep learning technique reliably. The author designs a multi-branch, neural network (MB-NN) model for automated extraction of major image areas and domain information features. He assesses the proposed model's efficacy with actual data sets and obtains a stronger 0.9151 [14], [15].

Noise removal is a key aspect in the domain of medical imaging. Retinal disease detections are one of the most important examples of image processing. Optical coherence tomography and Ultrasound image (retinal) is damaged by a little dot-like noise known as speckle noise. Several popular noise dismissal techniques are briefly reviewed and divided into different categories for diagnosing the growth of glaucoma [16].

The Genetic algorithm is used to calculate an optimal solution by pretending the evolution process of Bio in the selection of nature and genetic way. It has solid robustness, adaptability, fast convergence, and parallelism. It can be used in image segmentation to define the segmentation threshold. Their results were better by the Genetic algorithm than the old image segmentation [17], [18].

The author proposed a DEWO, a hybrid of the Differential Evolution with Whale Optimization for many level image segmentation by using the 2D histogram to achieve colorful image segmentation. The proposed work is equated with some heuristic algorithms using Tsallis, Renyi, and Kapur functions to confirm its effectiveness for different

entropy jobs. Results obtained from the planned image segmentation method are well compared to other meta-heuristic algorithms in each entropy-based segmentation done [19], [20].

The latest coronavirus of 2019 (COVID-19), centered in China, has spread rapidly to people residing in other countries. An automated detection device must, therefore, be introduced to prevent its spread among people. This paper suggested three separate models for diagnosing patients with coronavirus pneumonia, contaminated with chest x-ray radiation. The ResNet50 pre-trained Model provides 98 percent of its accuracy against the other two versions [21].

A pre-trained neural network (CNN) pre-trained system for the identification of exudates has been introduced. Data preprocessing is initially done to standardize exudate patches in the suggested solution. Fused features from fully attached (FC) layers are introduced into the SoftMax classifier. Two widely established publicly accessible repositories like aphthous and DIARETDB1 have been used to test the proposed system [22].

The cervixes of patients are listed as forms 1, 2, and 3. The model uses ResNet and Inception-V3, which had been pre-trained to meet the ImageNet Test. The findings suggest that the ResNet model is best conducted with top-down measurements. The Kaggle challenge takes the data set, including 1481 pictures, 512 pictures of the study, and 6734 more pictures [23], [24].

The ovaries play a key role in the female reproductive system since they form the egg or ovum required during fertilization. An inflated ovarian cyst can cause the disease to be twisted and infertile. The proposed study uses the standard VGG-16 model, which is well calibrated to our ultrasound images data set. The accuracy is obtained by 92.11 percentage, and exactness and failure curves for the proposed model are also suggested [25].

This paper uses state of the art neural networks in street and highway imagery throughout North America in marking photos. The research data used photos labeling hot, snowy, snow/ice, bad and offline for such tests. The tests evaluated various architectures of six convolution neural networks to evaluate their suitability to this issue. The size, consistency, and warning are calculated for increasing frame configuration for each frame. This question has been solved the EfficientNet-B4 implementation with a validation performance of 90.6 percent [26], [27].

A regional enhanced CNN (RECNN) for the object detection of remote sensing pictures is suggested. The RECNN combines the saliency maximum and multi-layer fusion technique into the CNN model. In particular, the saliency map is extracted and used for training the proposed model to improve saliency areas on the characteristic diagram. The proposed model is described in this article [28].

### A. Summary

This portion of the study discusses many attempts, advances, and achievements made by numerous previous researchers to address issues such as the description of Glaucoma condition issues. For classification purposes, different neural networks, artificial learning, data processing, and conventional computational approaches are explored, and numerous methods are used to forecast the diagnosis of glaucoma disorder. Different study techniques such as deep learning, artificial learning, and several other approaches have been utilized in the past by various researchers to diagnose Glaucoma disorder. What tests are good and exciting? This work would also suggest a hybrid deep learning model for the diagnosis of Glaucoma disease in which the findings of the Glaucoma disease assessment are further improved concerning precision.

## 3. RESEARCH METHODOLOGY

This section explains the methodology of the research work carried out in this research proposal. The flow of methodology of our proposed research is shown in "Fig. 3". The selected structure will show the idea of implementation of Inception-V3 and Vgg-16, which we have chosen to classify our data set.

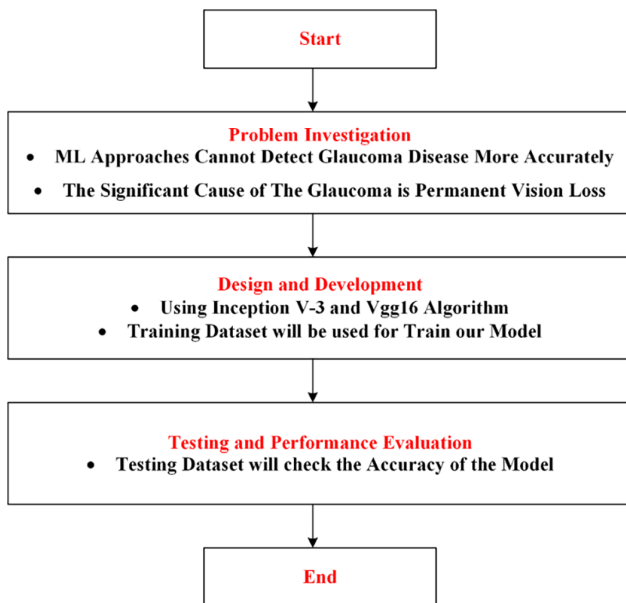


Figure 3. Proposed research framework

### A. Problem Investigation

The research work starts with the investigation of the problem given in the introduction section. The significant cause of glaucoma is permanent vision loss. In the literature, we have analyzed several machine learning approaches used by different researchers on fundus images. Some of the existing approaches to machine learning are C4.5, Naive Bayes Classifier, and Random Forest. These approaches cannot detect glaucoma disease more accurately. In this research, we have built an architecture based on the Deep

Learning technique, a CNN for Glaucoma disease detection. After analysis based on the accuracy, we evaluated which network is best for the detection—the deep learning techniques like CNN used for discriminating between non-glaucoma and glaucoma patterns for diagnostic decisions.

### B. Design and Development

In this section, the first step was labeling and then dividing the data set into the training data set and testing data set. In the second step, we made a Convolutional Neural Network with some layers, inputs in the form of images were passed through different layers for detecting pictures. In these layers, we made our CNN ignore the text in the given images and only given the picture as an output.

### C. Testing and Performance Evaluation

After the development of CNN, we ran it for input and tested its performance to ensure that it worked for the specific requirements. Furthermore, after taking the input from us, it took a little time on processing, as CNN utilizes GPU and produces the output in the form of an image ignoring the text.

### D. Data Collection

We have collected 508 fundus images that belong to 25 classes that come from the Joint Shantou International Eye Centre (JSIEC), Shantou city, Guangdong province, China. After downloading the images, we have applied the augmentation on the given data set and made 1563 images of the training and testing data set. The downloaded data set was not labeled, and for our analysis in deep learning, we need a labeled images data set. So, after augmentation, we have labeled all images with the class name of the disease. We have the following classes of the images: ['BRVO' 'CRVO' 'Chorioretinal Atrophy Coloboma' 'Congenital Disc Abnormality' 'Cotton Wool Spots' 'DR1' 'DR2' 'DR3' 'Disc Swelling and Elevation' 'Dragged Disc' 'Fibrosis' 'Fundus Neoplasm' 'Large Optic Cup' 'Laser Spots' 'Massive Hard Exudates' 'Myelinated Nerve Fiber' 'Normal' 'Peripheral Retinal Degeneration and Break' 'Preretinal Hemorrhage' 'Severe Hypertensive Retinopathy' 'Silicon Oil in Eye' 'Tessellated Fundus' 'Vessel Tortuosity' 'Vitreous Particles' 'Yellow White Spots Flecks'].

### E. Data Set

We have collected 508 fundus images that belong to 25 classes that come from the Joint Shantou International Eye Centre (JSIEC), Shantou city, Guangdong province, China. After downloading the images, we have applied the augmentation on the given data set and make the 1563 images of the training and testing dataset. The downloaded data set is not labeled, and for our analysis in deep learning, we have needed a labeled images data set. So, after augmentation, we have labeled all images with the class name of the disease.

### F. Resizing

Resizing is a processing in which we need to decrease or increase the number of pixels. Resizing refers to the scaling

of images. If you are resizing a picture, a new picture might be generated with a higher number of pixels or a lower number of pixels. There are two kinds of resizing one is zooming, and the other is shrinking. Zooming is how an image enlarged in the sense of details to become clearer and more visible. The image should be scaled in such a manner that it won't affect the image quality. Shrinking a picture means to delete the columns and rows of pixels that won't affect the picture's details. Before the resizing of the data set, we made a copy so that if anything bad happens to my data set, my research won't be affected and this is the main step that everybody should remember before going ahead because maybe they will not have that resource of data from where you have taken. We resized Inception-V3 Input size: [224\*224], and Vgg-16 input size: [224\*224] by python script run through CMD given the data set path. We made eleven data sets of that 1563 images and labeled them by a folder name, and we kept every image that was the same in the category.

#### G. Data Augmentation

It is a strategy seen in the Inception-V3 and Vgg-16 beginnings. It enables the data necessary for the training model to be directly expanded. It extends the training data set by using the same data set to construct modified image models. This ability allows Keras to respond to models by data augmentation in the deep learning neural network. Testing neural deep networks on additional data will best achieve professional models. The technique can generate variations of photos that improve models' fits to clarify what they have learned for the new images. This technique Keras profound learning libraries that match.

#### H. Inception-V3 Model

The Inception-V3 model we have used for the image recognition system consists of two parts: • With the Convolutional Neural Network (CNN), the feature extraction part • Classification part with SoftMax and fully connected layers The pre-prepared Inception-V3 Model accomplishes cutting edge exactness for perceiving general articles with

#### I. Vgg-16

Vgg-16, which was developed by Simonyan and Zisserman, is the champion at the 2014 ILSVRC competition. Vgg-16 consists of 16 convolution layers and has a very uniform design, which results in a direct result. models using the image data increase. This technique is usually used to train many neural networks, using the covering, cutting, and horizontal turn. For 2D images, mainly data increase is used. This method can be used to provide transformed image types.

#### J. Labeling

Multi-label image grouping is essential for neural networks, but this is a challenging task for data scientists. It is hard to make the relationship between a single with multi-label images [29]. Modern approaches to multi-label image classification can learn independent classifiers for

every category to classify input for results [30]. We have labeled my dataset into twenty-five categories, as shown in below "Fig. 4". 1000 classes, like Dishwasher, Dalmatian, and Zebra. The model concentrates general highlights from input pictures in the initial segment and arranges them dependent on those highlights in the next part. In move realizing, when we assemble another model to group our unique data set, we reuse the component extraction part and re-train the order part with our data set. Since we do not need to prepare the element extraction part (which is the most perplexing piece of the model), you can prepare the model with less computational assets and preparing time, as shown in below "Fig. 5".

Much like AlexNet, just 3x3 switches, but a ton of channels. It was made for 2-3 weeks on four GPUs. From now on, it was the network's favorite choice to remove highlights from images. The weight of the Vgg-16 is freely usable and has been seen as an extractor with several specific applications and difficulties. Vgg-16 consists, in any case, of 138 million parameters to be tested, as shown in below "Fig. 6".

## 4. RESULTS AND DISCUSSION

This section authorizes and tests the accuracy, performance, and accuracy further of the proposed method. Our model is often trained under supervision. That's why it needs manually labeled data. The convolutional layers are the same as VGG-16. The efficiency of our proposed model was evaluated by applying the ReLU function with three convolutional layers. ReLU and Batch normalization Function follows every convolutional layer. Two Fully-connected layers and two MaxPooling layers are used with an activation function named as SoftMax, SoftMax Layer

#### A. Preliminaries

Two essential measurement matrices for the model are emphasized in the analysis. First, it was a defeat, and second, a draw. The art databases are divided into 70 percent training and 30 percent test results. We used Colab to check and train the data set classification using 12 GB RAM Keras, Matplotlib, TensorFlow Sdk, NumPy Opencv, and imutils libraries. They were located on a Deep Network (DNN) platform, containing just one input layer, several hidden layers, and one output layer. The Inception-V3 and Vgg-16 variants have been tested.

#### B. Experiments Result

Different experiments are approved on two models, and these models are evaluated using accuracy and loss. The is the autoencoder with X classes that lets semantic segmentation distributes over X object classes for every pixel independently. The model was used for the data set of the old book scanned pages to classify it.

The data set was gained Glaucoma images of 25 classes. To make these pictures easy for the processing, we resolved Inception-V3 Input size: [224 X 224] and Vgg-16 input size: [224 X 224]. The data set included about 1563 images and

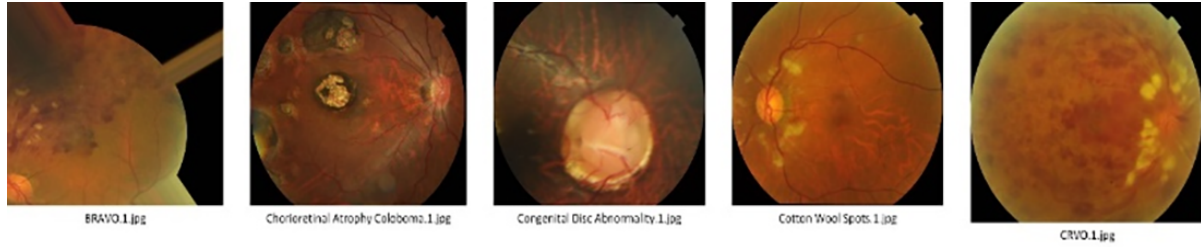


Figure 4. The sample images of the Glaucoma dataset

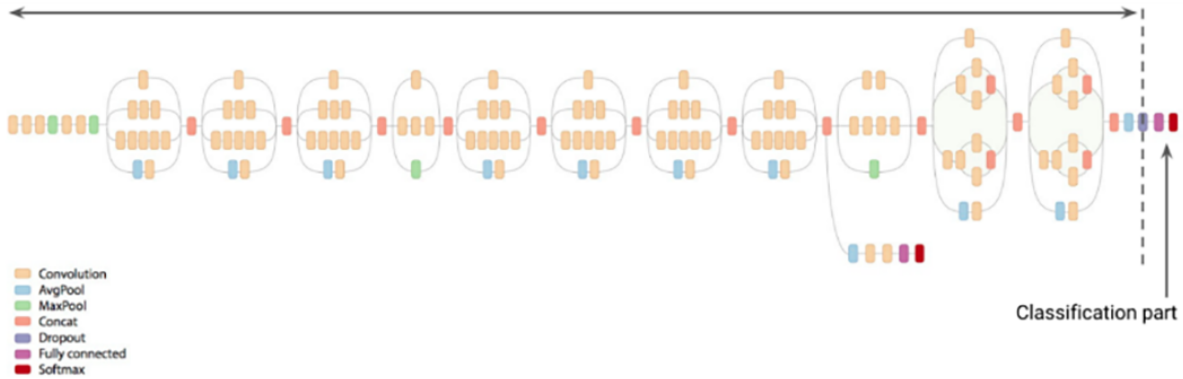


Figure 5. Feature Extraction Part of Inception-V3 Model



Figure 6. Architecture Diagram of Vgg-16

25 categories and was labeled in 11 data sets, as shown in below "Fig. 7". Following two methods are used throughout the simulation, such as our proposed method, Inception-V3 and Vgg-16. The training and testing experiments had performed on two algorithms, and the algorithm was valued by training accuracy and validation accuracy.

**C. Inception-V3 Model**

Batch Size: 30

Epoch: 10

Training Set 70 percent,

Testing Set 30 percent

Classes: ['BRVO' 'CRVO' 'Chorioretinal Atrophy Coloboma' 'Congenital Disc Abnormality' 'Cotton Wool Spots' 'DR1' 'DR2' 'DR3' 'Disc Swelling and Elevation' 'Dragged Disc' 'Fibrosis' 'Fundus Neoplasm' 'Large Optic Cup' 'Laser Spots' 'Massive Hard Exudates' 'Myelinated Nerve Fiber' 'Normal' 'Peripheral Retinal Degeneration

and Break' 'Preretinal Hemorrhage' 'Severe Hypertensive Retinopathy' 'Silicon Oil in Eye' 'Tessellated Fundus' 'Vessel Tortuosity' 'Vitreous Particles' 'Yellow White Spots Flecks'] as shown in "Fig. 7".

Image Input Size: 224 X 224

Optimizer: Adam With Learning Rate: 1e-3

1) Compiling Model

Giving the input dataset to the Inception-V3 model is the first step. The computational graph represents the dropout, and the type of layers are involved in the model. We have trained and tested the Inception-V3 model and measuring the performance based on loss and accuracy, as shown in "Table. 1".

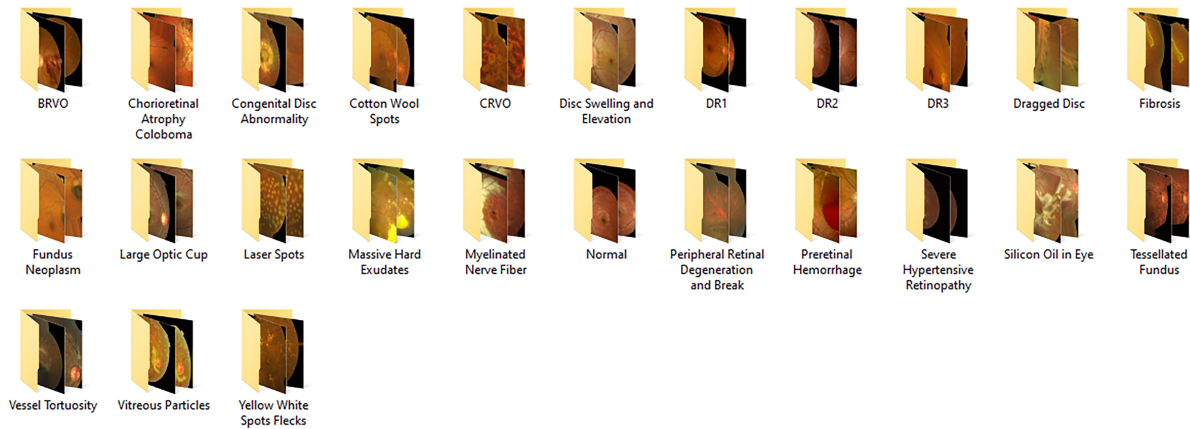


Figure 7. Labeling of my dataset

TABLE I. LOSS AND ACCURACY PERFORMANCE OF INCEPTION-V3 MODEL BY TRAINING AND TESTING DATA SET

Epoch	Loss	Val Accuracy
1	0.9710	0.9016
2	0.8732	0.8972
3	0.8154	0.9076
4	0.7763	0.8987
5	0.7499	0.8942
6	0.7309	0.8987
7	0.7127	0.9046
8	0.6963	0.9046
9	0.6810	0.8987
10	0.6694	0.9001

TABLE II. THE EVALUATED LOSS AND ACCURACY OF INCEPTION-V3 MODEL

Model name	Loss	Accuracy
1	0.6694	90.01

2) Classification Report

The Evaluated Loss and Accuracy of Inception-V3 Model by training and the testing data set is shown in "Table. 2".

"Table. 3" indicates the evaluation of results; it includes a precision, f1-score, and a recall based on the ten epochs. We have evaluated the performance of the Inception-V3 model based on these parameters. We have analyzed that the Inception-V3 model's accuracy is less on the first epoch, which is 90.16 percent, and after the steps of the epochs, the accuracy decreases to 90.01 percent. Also, the loss rate of the Inception-V3 model will decrease to 0.6694 from 0.9710. The training and testing loss and accuracy are shown in "Fig. 8".

TABLE III. CATEGORIES RESULT BY INCEPTION-V3

-	Precision	Recall	F1-Score
BRVO	0.84	0.86	0.85
CRVO	0.97	0.92	0.95
Choriorretinal Atrophy Coloboma	0.70	0.93	0.80
Congenital Disc Abnormality	0.96	1.00	0.98
Cotton Wool Spots	0.92	1.00	0.96
DR1	0.88	0.88	0.8
DR2	0.81	0.68	0.74
DR3	0.71	0.87	0.78
Disc Swelling and Elevation	0.96	0.92	0.94
Dragged Disc	1.00	0.96	0.98
Fibrosis	0.81	1.00	0.90
Fundus Neoplasm	1.00	0.79	0.88
Large Optic Cup	0.95	0.95	0.95
Laser Spots	1.00	0.89	0.94
Massive Hard Exudates	0.81	0.92	0.86
Myelinated Nerve Fiber	1.00	0.95	0.97
Normal	0.73	1.00	0.84
Peripheral Retinal Degeneration	1.00	0.90	0.95
Preretinal Hemorrhage	1.00	0.96	0.98
Severe Hypertensive Retinopathy	0.93	0.93	0.93
Silicon Oil in Eye	1.00	0.91	0.95
Tessellated Fundus	1.00	0.89	0.94
Vessel Tortuosity	0.94	0.94	0.94
Vitreous Particles	0.93	1.00	0.96
Yellow White Spots Flecks	0.64	0.47	0.55

The Inception-V3 model has a macro and weighted average based on the precision, recall, and F1-Score parameters, as shown in "Table. 4". The evaluated values of the macro and weighted average for precision is 90 percent and 91 percent, Also recall and F1-Score parameters are similar, which is 90 percent, 90 percent, and 90 percent, respectively, with the 90 percent accuracy.

D. Vgg-16 Model  
Batch Size: 30

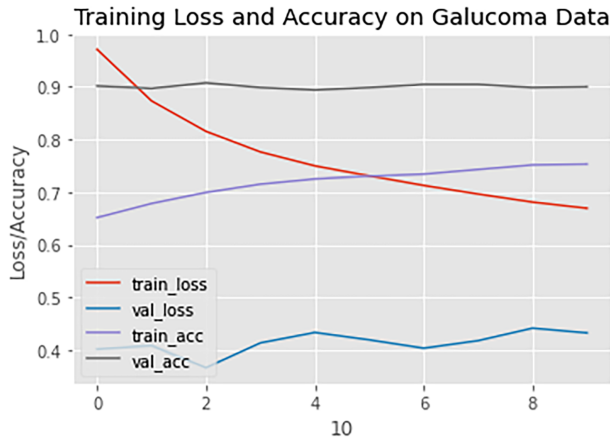


Figure 8. Inception-V3 Training and Testing Accuracy and loss

TABLE IV. AVERAGE EVALUATION PERFORMANCE OF INCEPTION-V3 MODEL ON TESTING DATA

Name	Precision	Recall	F1-score
Macro Avg	0.90	0.90	0.90
Weighted Avg	0.91	0.90	0.90
Accuracy	—	—	0.90

Epoch: 10

Training Set 70 percent, Testing Set 30 percent

Classes: ['BRVO' 'CRVO' 'Chorioretinal Atrophy Coloboma' 'Congenital Disc Abnormality' 'Cotton Wool Spots' 'DR1' 'DR2' 'DR3' 'Disc Swelling and Elevation' 'Dragged Disc' 'Fibrosis' 'Fundus Neoplasm' 'Large Optic Cup' 'Laser Spots' 'Massive Hard Exudates' 'Myelinated Nerve Fiber' 'Normal' 'Peripheral Retinal Degeneration and Break' 'Preretinal Hemorrhage' 'Severe Hypertensive Retinopathy' 'Silicon Oil in Eye' 'Tessellated Fundus' 'Vessel Tortuosity' 'Vitreous Particles' 'Yellow White Spots Flecks'] as shown in "Fig. 7".

Image Input Size: 224 X 224

Optimizer: Adam With Learning Rate: 1e-3

#### 1) Compiling Model

Giving the input data set to the Vgg-16 model is the first step. The computational graph represents the dropout, and the type of layers are involved in the model. We have trained and tested the Vgg-16 model and measuring the performance based on loss and accuracy, as shown in "Table. 5"

#### 2) Classification Report

The Evaluated Loss and Accuracy of Vgg-16 Model by training and the testing dataset is shown in "Table. 6".

TABLE V. LOSS AND ACCURACY PERFORMANCE OF VGG-16 MODEL BY TRAINING AND TESTING DATASET

Epoch	Loss	Val Accuracy
1	1.0033	0.7809
2	0.8914	0.8003
3	0.8187	0.8107
4	0.7644	0.8167
5	0.7223	0.8227
6	0.6861	0.8241
7	0.6601	0.8212
8	0.6388	0.8256
9	0.6098	0.8301
10	0.6008	0.8346

TABLE VI. THE EVALUATED LOSS AND ACCURACY OF VGG-16 MODEL

Model name	Loss	Accuracy
Vgg-16	0.6008	83.46

"Table. 7" indicates the evaluation of results; it includes a precision, f1-score, and a recall based on the ten epochs. We have evaluated the performance of the Vgg-16 model based on these parameters. We have analyzed that the Vgg-16 model's accuracy is less on the first epoch, which is 78.09 percent, and after the steps of the epochs, the accuracy increases to 83.46 percent. Also, the loss rate of the Vgg-16 model will decrease to 1.0033 from 0.6008. The training and testing loss and accuracy are shown in "Fig. 9".

The Vgg-16 model has a macro and weighted average based on the precision, recall, and F1-Score parameters, as shown in "Table. 8". The evaluated values of the macro and weighted average for precision is 90 percent and 91 percent, Also recall and F1-Score parameters are similar, which is 90 percent, 90 percent, and 90 percent, respectively, with

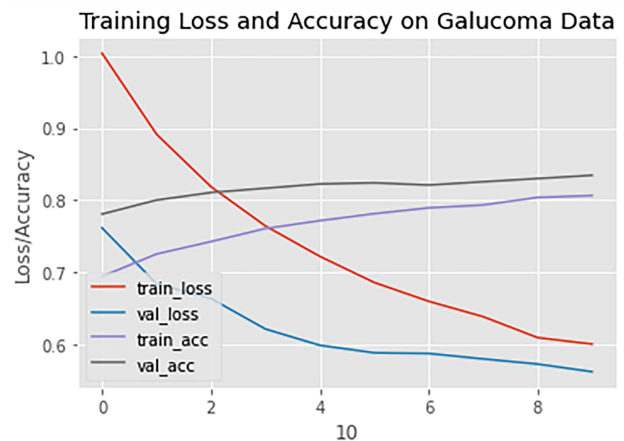


Figure 9. Vgg-16 Training and Testing Accuracy and loss





TABLE VII. CATEGORIES RESULT BY VGG-16

-	Precision	Recall	F1-Score
BRVO	0.64	0.49	0.55
CRVO	0.89	0.89	0.89
Chorioretinal Atrophy			
Coloboma	1.00	0.80	0.89
Congenital Disc Abnormality	0.88	0.88	0.88
Cotton Wool Spots	0.88	0.88	0.88
DR1	1.00	0.88	0.94
DR2	0.67	0.78	0.72
DR3	0.53	0.70	0.60
Disc Swelling and Elevation	0.92	0.96	0.94
Dragged Disc	0.91	0.87	0.89
Fibrosis	0.80	0.91	0.85
Fundus Neoplasm	0.88	0.75	0.81
Large Optic Cup	0.62	0.65	0.63
Laser Spots	1.00	0.93	0.96
Massive Hard Exudates	0.83	0.79	0.81
Myelinated Nerve Fiber	0.79	0.79	0.79
Normal	0.59	0.92	0.72
Peripheral Retinal Degeneration	0.91	1.00	0.95
Preretinal Hemorrhage	0.96	0.96	0.96
Severe Hypertensive Retinopathy	0.93	0.93	0.93
Silicon Oil in Eye	0.97	0.94	0.96
Tessellated Fundus	0.81	0.72	0.76
Vessel Tortuosity	0.92	0.94	0.93
Vitreous Particles	0.92	0.88	0.90
Yellow White Spots Flecks	0.67	0.42	0.52

TABLE VIII. AVERAGE EVALUATION PERFORMANCE OF INCEPTION-V3 MODEL ON TESTING DATA

Name	Precision	Recall	F1-score
Macro Avg	0.84	0.83	0.83
Weighted Avg	0.84	0.83	0.83
Accuracy	—	—	0.83

the 90 percent accuracy.

*E. Summary*

In this section, we have discussed our dataset results, which were resized and labeled into 25 categories. This dataset was divided into trained, which was about 70 percent, and testing was about 30 percent for our Machines. We tested two methods and compared them for accuracy, and we got that our proposed methods, which are Inception-V3, brought better results than Vgg-16. The testing accuracy of Inception-V3 was about 90.01 percent with 0.6694 loss, and the Vgg-16 had 83.46 percent with 0.6008 loss. The

TABLE IX. THE STATISTICAL COMPARISON OF INCEPTION-V3 AND VGG-16 MODEL BASED ON LOSS AND ACCURACY

Model Name	Loss	Accuracy
Inception-V3	0.6694	90.01
Vgg-16	0.6008	83.46

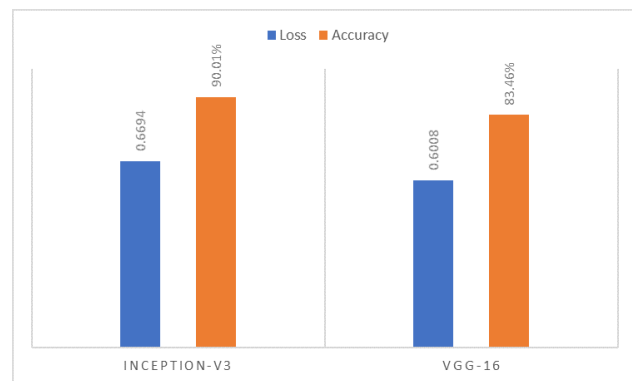


Figure 10. The bar chart visualization of Inception-V3 and VGG-16 model based on loss and accuracy

result of Inception-V3 was better, and the reason is, it has a more convolutional layer than Vgg-16. The statistical results and the bar chart visualization are shown in "Fig. 10" "Table. 9".

**5. CONCLUSION**

Before that, too many models of Neural Networks segmentation were planned. Many computer scientists have done some research to boost the classification performance, but the precision of such Artificial Neural Networks is still missing. That's why we've suggested the Invention V-3 approach for image classification based on Convolution Neural Networks. The model we have developed has the potential to address this CNN model's problem of classification accuracy. Experimental findings in our study were focused on two versions, Inception-V3 and Vgg-16. After the simulation, we got comparatively better results regarding accuracy and loss on Inception-V3 than Vgg-16. The achieved objectives are described in the next segment. In this paper, we have used the Google Co-Lab for our analysis, and for this, we have access to the limited RAM; that's why we cannot perform well.

**6. FUTURE WORK**

In the future, we will get our mini supercomputer machine and more images for our analysis. We will also use different latest neural networks to compare with the old one, which we have already used. For achieving this goal perfectly, further research and improvement in the current work are outlined in the following future work.

- Increasing the number of images in the data set will give high accuracy than previous.



- We will evaluate the performance of other neural networks on the given data set.
- By creating an application that can track the history of each glaucoma on the website.

## REFERENCES

- [1] N. M. Zaitoun and M. J. Aqel, "Survey on image segmentation techniques," *Procedia Computer Science*, vol. 65, pp. 797–806, 2015.
- [2] R. G. Schneider and T. Tuytelaars, "Example-based sketch segmentation and labeling using crfs," *ACM Transactions on Graphics (TOG)*, vol. 35, no. 5, pp. 1–9, 2016.
- [3] J. R. Uijlings, K. E. Van De Sande, T. Gevers, and A. W. Smeulders, "Selective search for object recognition," *International journal of computer vision*, vol. 104, no. 2, pp. 154–171, 2013.
- [4] P. Sermanet, D. Eigen, X. Zhang, M. Mathieu, R. Fergus, and Y. LeCun, "Overfeat: Integrated recognition, localization and detection using convolutional networks," *arXiv preprint arXiv:1312.6229*, 2013.
- [5] D. Chai and K. N. Ngan, "Face segmentation using skin-color map in videophone applications," *IEEE Transactions on circuits and systems for video technology*, vol. 9, no. 4, pp. 551–564, 1999.
- [6] F. Schroff, D. Kalenichenko, and J. Philbin, "Facenet: A unified embedding for face recognition and clustering," in *Proceedings of the IEEE conference on computer vision and pattern recognition*, 2015, pp. 815–823.
- [7] C. B. Anusorn, W. Kongprawechnon, T. Kondo, S. Sintuwong, and K. Tungpimolrut, "Image processing techniques for glaucoma detection using the cup-to-disc ratio," *Science & Technology Asia*, pp. 22–34, 2013.
- [8] M. K. Dutta, A. K. Mourya, A. Singh, M. Parthasarathi, R. Burget, and K. Riha, "Glaucoma detection by segmenting the super pixels from fundus colour retinal images," in *2014 international conference on medical imaging, m-health and emerging communication systems (MedCom)*. IEEE, 2014, pp. 86–90.
- [9] F. Khan, S. A. Khan, U. U. Yasin, I. ul Haq, and U. Qamar, "Detection of glaucoma using retinal fundus images," in *The 6th 2013 Biomedical Engineering International Conference*. IEEE, 2013, pp. 1–5.
- [10] A. Li, J. Cheng, D. W. K. Wong, and J. Liu, "Integrating holistic and local deep features for glaucoma classification," in *2016 38th Annual International Conference of the IEEE Engineering in Medicine and Biology Society (EMBC)*. IEEE, 2016, pp. 1328–1331.
- [11] B. Al-Bander, W. Al-Nuaimy, M. A. Al-Tae, and Y. Zheng, "Automated glaucoma diagnosis using deep learning approach," in *2017 14th International Multi-Conference on Systems, Signals & Devices (SSD)*. IEEE, 2017, pp. 207–210.
- [12] T. Saba, S. T. F. Bokhari, M. Sharif, M. Yasmin, and M. Raza, "Fundus image classification methods for the detection of glaucoma: A review," *Microscopy research and technique*, vol. 81, no. 10, pp. 1105–1121, 2018.
- [13] M. R. C. LOUHDI and H. BEHJA, "Ontology learning from relational databases: Transforming recursive relationships to owl components," *Int. J. Adv. Comput. Sci. Appl.*, vol. 10, no. 10, pp. 265–270, 2019.
- [14] Y. Chai, H. Liu, and J. Xu, "Glaucoma diagnosis based on both hidden features and domain knowledge through deep learning models," *Knowledge-Based Systems*, vol. 161, pp. 147–156, 2018.
- [15] B. Ahmad, "Intelligent digital twin to make robot learn the assembly process through deep learning," *LGURJCSIT*, vol. 5, no. 3, pp. 65–72, 2021.
- [16] S. Sahu, H. V. Singh, B. Kumar, A. K. Singh, and P. Kumar, "Image processing based automated glaucoma detection techniques and role of de-noising: a technical survey," in *Handbook of Multimedia Information Security: Techniques and Applications*. Springer, 2019, pp. 359–375.
- [17] C. Tan, Y. Sun, G. Li, B. Tao, S. Xu, and F. Zeng, "Image segmentation technology based on genetic algorithm," in *Proceedings of the 2019 3rd International Conference on Digital Signal Processing*, 2019, pp. 27–31.
- [18] H. Nisar, B. Wajid, S. Shahid, F. Anwar, I. Wajid, A. Khatoun, M. U. Sattar, and S. Sadaf, "Whole-genome sequencing as a first-tier diagnostic framework for rare genetic diseases," *Experimental Biology and Medicine*, p. 153537022111040046, 2021.
- [19] G. Vig, S. Varshney, S. Kumar, and M. Shahbaz, "Entropy-based multilevel 2d histogram image segmentation using dewo optimization algorithm," in *2019 International Conference on Automation, Computational and Technology Management (ICACTM)*. IEEE, 2019, pp. 206–212.
- [20] Z. Zahid, M. U. Sattar, H. W. Khan, A. Zahid, and M. F. Riaz, "A smart analysis and visualization of the power forecasting in pakistan," *International Journal of Computing and Digital Systems*, vol. 10, 2021.
- [21] A. Narin, C. Kaya, and Z. Pamuk, "Automatic detection of coronavirus disease (covid-19) using x-ray images and deep convolutional neural networks," *Pattern Analysis and Applications*, pp. 1–14, 2021.
- [22] M. Mateen, J. Wen, N. Nasrullah, S. Sun, and S. Hayat, "Exudate detection for diabetic retinopathy using pretrained convolutional neural networks," *Complexity*, vol. 2020, 2020.
- [23] M. Arora, S. Dhawan, and K. Singh, "Exploring deep convolution neural networks with transfer learning for transformation zone type prediction in cervical cancer," in *Soft Computing: Theories and Applications*. Springer, 2020, pp. 1127–1138.
- [24] M. Narmeen, M. U. Sattar, M. Fatima, H. W. Khan, M.-u.-D. Azad, and F. Ghani, "Impact of weather on covid-19 in metropolitan cities of pakistan: A data-driven approach," *International Journal of Computing and Digital System*, 2021.
- [25] S. Srivastava, P. Kumar, V. Chaudhry, and A. Singh, "Detection of ovarian cyst in ultrasound images using fine-tuned vgg-16 deep learning network," *SN Computer Science*, vol. 1, no. 2, pp. 1–8, 2020.
- [26] S. Ramanna, C. Sengoz, S. Kehler, and D. Pham, "Near real-time map building with multi-class image set labeling and classification of road conditions using convolutional neural networks," *Applied Artificial Intelligence*, pp. 1–31, 2021.
- [27] A. Ghaffar, S. Alanazi, M. Alruwaili, M. U. Sattar, W. Ali, M. Hu-

mayun, S. Y. Siddiqui, F. Ahmad, and M. A. Khan, "Multi-stage intelligent smart lockdown using sir model to control covid 19," *Intelligent Automation and Soft Computing*, pp. 429–445, 2021.

- [28] J. Lei, X. Luo, L. Fang, M. Wang, and Y. Gu, "Region-enhanced convolutional neural network for object detection in remote sensing images," *IEEE Transactions on Geoscience and Remote Sensing*, vol. 58, no. 8, pp. 5693–5702, 2020.
- [29] F. Zhu, H. Li, W. Ouyang, N. Yu, and X. Wang, "Learning spatial regularization with image-level supervisions for multi-label image classification," in *Proceedings of the IEEE Conference on Computer Vision and Pattern Recognition*, 2017, pp. 5513–5522.
- [30] J. Wang, Y. Yang, J. Mao, Z. Huang, C. Huang, and W. Xu, "Cnn-rnn: A unified framework for multi-label image classification," in *Proceedings of the IEEE conference on computer vision and pattern recognition*, 2016, pp. 2285–2294.



**Fatima Ghani** has done a BS in Computer Sciences and is currently enrolled in MS Data Science at the University of Management and Technology, Lahore. She is also working as a Data Analyst at the Directorate of General Health Services, Punjab, Lahore. She has a good and sound knowledge of data analysis and large-scale data reporting, especially in the health sector. Her research interest includes Deep Learning, Machine

learning, Data Analysis, and Data Reporting.



**Usman Sattar** has more than fifteen years of teaching, training, and consultancy experience in the fields of Information System especially Immersive Technologies, Data Science, and Enterprise Systems System Security. He is PhD (Informatics) – Scholar at Malaysia University of Science and Technology, Malaysia.



**Hamza Wazir Khan** has seven years of diversified experience in field of Information System and Marketing. Currently, he is working as a Lecturer in Information System Department at University of Management, Lahore and Technology. He has given his services in form of teaching, trainings, and consultancy in fields of Data Science, Digital Marketing, Enterprise Resource Planning, and E Business.



**Mehak Narmeen** has completed MS Data Science from the University of Management and Technology, Lahore, Pakistan. At present, she is also working as a Senior Software Engineer in a private software house. She has strong programming skills and even a mentor to her juniors. She has participated and won multiple coding competitions across the country. She has been a UGRAD scholarship holder and spent a semester as

an exchange student at Murray State University, KY, USA. Her research interests include Machine Learning, IoT, Enterprise Resource Planning, and Data Analysis.



**Ahsan Mehmood** has done BS honors. In Computer Science currently doing MS Information Technology from Central Queensland University, Melbourne Australia. He has good programming skills in different languages. He is also working as Software Developer at Ozean Pty LTD. His interests include Android development, web development, Database Data Analysis